

---

# Weak Information Transfer between Non-Matching Warped Interfaces

Thomas Dickopf and Rolf Krause

University of Bonn, Institute for Numerical Simulation  
Wegelerstraße 6, 53115 Bonn, Germany  
{dickopf,krause}@ins.uni-bonn.de

**Summary.** We consider the information transfer between non-matching finite element meshes arising from domain decomposition. Dealing with complex three-dimensional geometries, especially in the case of computational mechanics and nonlinear contact problems, one can usually not achieve a decomposition of the global domain with mere planar interfaces in a sensible way. Thus, subdomains with warped interfaces emerge which, after an independent discretization, yield a geometrically non-conforming decomposition with small gaps and overlaps. In this paper, we employ a mortar approach and develop a method for the assembly of a discrete coupling operator providing a stable information transfer across such geometrically distinct warped interfaces.

## 1 Introduction

The efficient realization of an exchange of discrete information between geometrically non-conforming interfaces in three-dimensional space is of high interest in many applications. In case a domain is decomposed, even if the real boundaries of the subdomains coincide, the discrete interior interfaces formed by independently generated meshes will not. Besides, in computational mechanics often the use of an a priori decomposition into structural parts with different mechanical properties is advisable. This specifically holds true for contact problems, where the actual interface is unknown in advance.

In this paper, the discretization of the coupling constraints is done in a weak sense by a mortar approach [2], proposing the use of an  $L^2$ -projection between non-matching meshes to allow for optimal error estimates. Here, motivated by [4, 8, 9], we develop an efficient method to compute the emerging discrete transfer operator for meshes on warped interfaces exhibiting gaps and overlaps. The whole extent of its applicability becomes clear when we use our operator to simulate the transmission of forces between colliding bodies.

## 2 Discrete Information Transfer

Let  $\Gamma^k$ ,  $k \in \{m, s\}$ , be a two-dimensional connected submanifold of  $\mathbb{R}^3$  with boundary. In applications each of these surfaces naturally appears as a subset of the boundary of a three-dimensional domain  $\Omega^k$ ,  $k \in \{m, s\}$ . In particular, it is assumed that all the surface information exchange between the domains  $\Omega^m$  and  $\Omega^s$  takes place across the segments  $\Gamma^m$  and  $\Gamma^s$ . For simplicity we do not consider crosspoints of more than two interfaces.

In order to prescribe matching conditions expressing the mutual information transfer, we assume a sufficiently smooth, bijective mapping  $\Phi : \Gamma^s \rightarrow \Gamma^m$  to be given, which relates the opposite interfaces. Although, in general, such a mapping is part of the overall solution and not achievable a priori, a reasonable discrete version reflecting coupling in normal direction can be found by a linearization, which we discuss later on. Then, for a Sobolev function  $u = (u^m, u^s) \in \prod_{k \in \{m, s\}} H^{\frac{1}{2}}(\Gamma^k)$ , emerging as the respective traces of  $H^1$ -functions defined on  $\Omega^k$ ,  $k \in \{m, s\}$ , the transmission conditions which for second order partial differential equations commonly have to be realized are

$$[u] = 0, \quad \frac{\partial u^m}{\partial \mathbf{n}} \circ \Phi = \frac{\partial u^s}{\partial \mathbf{n}}, \quad \text{a. e. on } \Gamma^s. \quad (1)$$

Here,  $[u] := u^s - u^m \circ \Phi$  is the jump of  $u$  across the interface  $\Gamma := \Gamma^m \cup \Gamma^s$  and  $\frac{\partial}{\partial \mathbf{n}}$  denotes the appropriate normal derivative on  $\Gamma$ .

The enforcement of discrete constraints corresponding to (1), which we present now, is motivated by the understanding that, in a very general sense, with non-matching meshes a pointwise coupling yields indeed a conforming approximation but does not provide optimal discretization error estimates. So, we employ a mortar approach, see [2], and impose a weak matching condition by the introduction of suitable Lagrange multipliers on the interface.

Let  $\mathcal{T}^k$  be a shape regular surface mesh of  $\Gamma^k$ ,  $k \in \{m, s\}$ , made up of triangles and quadrilaterals. In applications these meshes are inherited from unstructured volume meshes of the domains  $\Omega^m$  and  $\Omega^s$ , consisting of tetrahedrons, hexahedrons, pyramids, and prisms. We denote the nodes of  $\mathcal{T}^k$  by  $\mathcal{N}^k$ . On both surface meshes, we use the space of Lagrangian conforming finite elements of first order  $X_h(\Gamma^k)$  and denote its nodal basis functions as  $(\lambda_p^k)_{p \in \mathcal{N}^k}$  with  $\lambda_p^k(q) = \delta_{pq}$ ,  $p, q \in \mathcal{N}^k$ ,  $k \in \{m, s\}$ . Then, the unconstrained product finite element space is given as  $X_h := \prod_{k \in \{m, s\}} X_h(\Gamma^k)$ . All finite element functions will be marked by the subscript  $h$ .

We define a discrete multiplier space  $M_h \subseteq X_h(\Gamma^s)$  and fix a basis  $(\psi_p)_{p \in \mathcal{N}^s}$ . In fact,  $M_h$  turns out to be an approximation space for the normal derivative on  $\Gamma$  and has to be chosen compatibly. Because the multiplier space is associated with the mesh  $\mathcal{T}^s$  and because the values on  $\Gamma^m$  will constrain the values on  $\Gamma^s$ , we call entities with superscript  $s$  slave (or non-mortar), whereas entities with superscript  $m$  are referred to as master (or mortar). Then, the well-known weak “zero jump condition” of the mortar method from [2] is

$$\int_{\Gamma^s} \psi_h \cdot [u_h] d\mathbf{a} = 0 \quad \forall \psi_h \in M_h.$$

Inspired by these weak coupling constraints, we use the representations of  $u_h$  and  $\psi_h$  in the chosen bases of  $X_h$  and  $M_h$ , respectively, and define the discrete mortar transfer operator via its algebraic representation,  $\mathbf{T} := \mathbf{D}^{-1}\mathbf{B}$ , with the entries

$$\begin{aligned} d_{pq} &:= \int_{\Gamma^s} \psi_p \lambda_q^s d\mathbf{a}, & p, q \in \mathcal{N}^s, \\ b_{pq} &:= \int_{\Gamma^s} \psi_p (\lambda_q^m \circ \Phi) d\mathbf{a}, & p \in \mathcal{N}^s, q \in \mathcal{N}^m. \end{aligned} \quad (2)$$

The transfer operator  $\mathbf{T}$  maps discrete values on the master side via the multiplier space  $M_h$  to the slave side. More precisely, for  $v^m \in X_h(\Gamma^m)$  the function  $\mathbf{T}v^m$  is the  $L^2$ -projection of  $v^m \circ \Phi$  onto  $X_h(\Gamma^s)$ . Now, two possible algebraic forms of the discrete matching conditions are

$$(\mathbf{D}u_h^s)_p - (\mathbf{B}u_h^m)_p = 0 \quad \text{or} \quad (u_h^s)_p - (\mathbf{T}u_h^m)_p = 0 \quad \forall p \in \mathcal{N}^s. \quad (3)$$

The left variant (3)<sub>1</sub> can be used as a constraint in the saddle point formulation of a coupled problem. The right one (3)<sub>2</sub> allows for either the elimination of the degrees of freedom on the slave side or the application of a Dirichlet–Neumann type algorithm as in [4]. Note that the approach is indeed non-conforming, i.e. the weak coupling constraints (3) do generally not guarantee that the stronger condition (1) is satisfied.

The constraints involving the mortar transfer operator  $\mathbf{T}$  can easily be adjusted for the approximation of a variational inequality, e.g., stemming from a free boundary value problem. If  $\mathbf{D}$  is a diagonal matrix with positive entries, which can be achieved by using dual Lagrange multipliers as in [6, 7] or mass lumping, this results in ordinary inequality constraints for all  $p \in \mathcal{N}^s$ . Naturally, our coupling approach is not limited to scalar valued problems.

Finally, to prove optimal discretization error estimates for the global approximation of the considered problem, all discrete function spaces have to be chosen appropriately. In particular, a uniform inf-sup condition between the finite element spaces on  $\Omega^m$  and  $\Omega^s$  and the multiplier space  $M_h$  needs to hold. Then, a proof can be carried out following [2] in case of a linear problem and following [7] in case of a free boundary value problem.

### 3 The Discrete Coupling Operator

Even in the case of matching interfaces (but possibly non-matching meshes) the assembly of the master-slave coupling is intricate because intersections of arbitrary element faces have to be computed. But dealing with geometrically non-conforming decompositions exhibiting gaps and overlaps between warped interfaces, we are obliged to meet further challenges, since the unknown mapping  $\Phi$  directly enters the definition of the transfer operator in (2). A first idea for the handling of this more sophisticated case by projecting the meshes of the opposite interfaces onto an explicitly given two-dimensional submanifold of  $\mathbb{R}^3$  can be found in [4]. In [9] the

interfaces are projected onto a plane varying with the slave side, instead. Then, the coupling terms are computed by numerical integration on intersections of projected faces in this plane. A further possibility is the automatic construction of an approximate identifying mapping  $\Phi_h$  as in [8].

Here, we derive an algorithm, which assembles the discrete coupling operator from local information exclusively. We compute triangulated intersections of two respective faces in a locally adjusted projection plane but, unlike before, carry out the quadrature on the possibly warped slave side  $\Gamma^s$  directly. Going beyond [9], we give a sound derivation of our element-based approach, which does not use any parametrizations of the two-dimensional faces and is also suitable for isoparametric elements.

Let  $\mathcal{F}^m$  and  $\mathcal{F}^s$  be the sets of master and slave faces, respectively. Only to ease the derivation of the algorithm, we assume a bounded set  $U \subset \mathbb{R}^2$  and global parametrizations  $\varphi_k : U \rightarrow \Gamma^k$  of  $\Gamma^k$ ,  $k \in \{m, s\}$ , to be given so that  $\Phi = \varphi_m \circ \varphi_s^{-1}$ . This means that points on the interfaces which have the same preimages in the parameter domain  $U$  are identified. We point out that the parametrizations will shortly be replaced by suitable discrete and local versions, which are immediately computable from the geometric information already available in finite element programs.

In the following, we denote the three-dimensional element belonging to the face  $F^k$  from the mesh  $\mathcal{T}^k$  by  $E^k$ . We generically denote the respective reference element of  $E^m$  and  $E^s$  by  $\hat{E}$ . The coordinate transformation from  $\hat{E}$  to  $E^k$  is called  $\mathbf{G}_{\hat{E} \rightarrow E^k}$  and the affine transformation between two triangles  $T_1$  and  $T_2$  is  $\mathbf{G}_{T_1 \rightarrow T_2}$ .

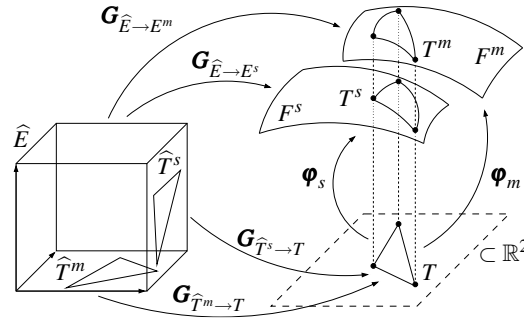


**Fig. 1.** Derivation of the assembly algorithm for the discrete coupling operator.

We use the decompositions of  $\Gamma^m$  and  $\Gamma^s$  induced by the meshes  $\mathcal{T}^m$  and  $\mathcal{T}^s$  and observe the fact that the set  $\{\Phi^{-1}(F^m) \mid F^m \in \mathcal{F}^m\}$  is a partition of the slave side  $\Gamma^s$ . In particular, for each slave face  $F^s \in \mathcal{F}^s$  we have  $\cup_{F^m \in \mathcal{F}^m} (F^s \cap (\varphi_s \circ \varphi_m^{-1})(F^m)) = F^s$ . Then, integrating by substitution, we write formally,

$$\begin{aligned}
b_{pq} &= \sum_{\substack{F^s \in \mathcal{F}^s \\ F^m \in \mathcal{F}^m}} \left( \int_{F^s \cap (\boldsymbol{\varphi}_s \circ \boldsymbol{\varphi}_m^{-1})(F^m)} \boldsymbol{\psi}_p \cdot (\boldsymbol{\lambda}_q^m \circ \boldsymbol{\varphi}_m \circ \boldsymbol{\varphi}_s^{-1}) d\mathbf{a} \right) \\
&= \sum_{\substack{F^s \in \mathcal{F}^s \\ F^m \in \mathcal{F}^m}} \left( \int_{\boldsymbol{\varphi}_s^{-1}(F^s) \cap \boldsymbol{\varphi}_m^{-1}(F^m)} (\boldsymbol{\psi}_p \circ \boldsymbol{\varphi}_s) \cdot (\boldsymbol{\lambda}_q^m \circ \boldsymbol{\varphi}_m) \cdot |\det \nabla \boldsymbol{\varphi}_s| d\mathbf{a} \right).
\end{aligned}$$

We now assume that each intersection  $\boldsymbol{\varphi}_s^{-1}(F^s) \cap \boldsymbol{\varphi}_m^{-1}(F^m) \subset \mathbb{R}^2$  can be divided into finitely many triangles, and for each triangle  $T$  we denote the corresponding triangles on the interfaces by  $T^k := \boldsymbol{\varphi}_k(T)$ ,  $k \in \{m, s\}$ , see Fig. 1 in case  $E^m$  and  $E^s$  are hexahedrons. Then, we transfer the triangles to the reference element with the inverses of the three-dimensional transformations, namely  $\hat{T}^k := \mathbf{G}_{\hat{E} \rightarrow E^k}^{-1}(T^k)$ . Now the two-dimensional affine transformations  $\mathbf{G}_{\hat{T}^k \rightarrow T}$  from these triangles  $\hat{T}^k$  to the triangle  $T$  can easily be computed. Hence, we have  $\boldsymbol{\varphi}_k|_T \equiv \mathbf{G}_{\hat{E} \rightarrow E^k} \circ \mathbf{G}_{\hat{T}^k \rightarrow T}^{-1}$  and are in a position to continue the above formal calculation for the contribution of each triangle  $T$  separately,

$$\begin{aligned}
&\int_T (\boldsymbol{\psi}_p \circ \boldsymbol{\varphi}_s) \cdot (\boldsymbol{\lambda}_q^m \circ \boldsymbol{\varphi}_m) \cdot |\det \nabla \boldsymbol{\varphi}_s| d\mathbf{a} = \\
&|\det \nabla \mathbf{G}_{\hat{T}^s \rightarrow T}^{-1}| \int_T (\hat{\boldsymbol{\psi}}_p \circ \mathbf{G}_{\hat{T}^s \rightarrow T}^{-1}) \cdot (\hat{\boldsymbol{\lambda}}_q \circ \mathbf{G}_{\hat{T}^m \rightarrow T}^{-1}) \cdot |\det \nabla \mathbf{G}_{\hat{E} \rightarrow E^s}(\mathbf{G}_{\hat{T}^s \rightarrow T}^{-1})| d\mathbf{a}. \quad (4)
\end{aligned}$$

At this we use the representations via the shape functions on the reference element,  $\boldsymbol{\psi}_p \circ \mathbf{G}_{\hat{E} \rightarrow E^s} = \hat{\boldsymbol{\psi}}_p$  and  $\boldsymbol{\lambda}_q^m \circ \mathbf{G}_{\hat{E} \rightarrow E^m} = \hat{\boldsymbol{\lambda}}_q$ . By abuse of notation  $\nabla \mathbf{G}_{\hat{E} \rightarrow E^s}$  stands for its restriction to the corresponding faces in the domain  $\hat{E}$  and the codomain  $E^s$ , respectively. Thus, the exclusive use of the three-dimensional finite element transformations supersedes the additional introduction of two-dimensional parametrizations of warped faces. Besides, we note that  $|\det \nabla \mathbf{G}_{\hat{T}^s \rightarrow T}^{-1}| = \frac{|\hat{T}^s|}{|T|}$  is constant because  $\mathbf{G}_{\hat{T}^s \rightarrow T}$  is an affine mapping.

These considerations lead to the understanding that the entries  $b_{pq}$  of the coupling matrix  $\mathbf{B}$  can be computed as a sum of integrals of the form (4) over triangles. This requires that suitable approximations of the parametrizations  $\boldsymbol{\varphi}_k$  are known. In fact there is no need to establish any parametrizations explicitly. We only have to replace all triangles  $T$ ,  $T^m$ , and  $T^s$  by approximating ones to allow for the evaluation of the right hand side of (4). For this purpose, we introduce the following algorithm. Firstly, the intersections and their triangulations are computed in a projection plane locally adjusted to the slave side. Secondly, the triangles  $T^m$  and  $T^s$  on the respective interfaces  $\Gamma^m$  and  $\Gamma^s$  are created by an inverse projection. Then, an appropriate quadrature formula can be applied on the respective reference elements directly.

### Algorithm

- (A1) Build an octree data structure to determine which master and slave faces are “close” to each other.
- (A2) Loop over all slave faces  $F^s \in \mathcal{F}^s$ .

- (B1) Loop over all master faces  $F^m \in \mathcal{F}^m$ .
  - (C1) Only continue if  $F^m$  is “close” to  $F^s$ .
  - (C2) Apply a Householder reflection  $H$  so that  $H(\mathbf{n}^s) = \mathbf{e}_3$ , where  $\mathbf{n}^s$  is a suitably chosen outer normal of the current slave face.
  - (C3) Compute  $\tilde{F}^k$  as the convex hull of the corners of  $F^k$  projected onto the  $\mathbf{e}_1\mathbf{e}_2$ -plane,  $k \in \{m, s\}$ .
  - (C4) Compute the intersection  $\tilde{F}^m \cap \tilde{F}^s$  and a triangulation  $\cup T_i$ .
  - (C5) Loop over all triangles  $T_i$ .
    - (D1) Perform an inverse projection of the corners of  $T_i$  to get corresponding triangles  $T_i^m$  and  $T_i^s$  on the original faces  $F^m$  and  $F^s$ , respectively.
    - (D2) Use the transformation  $\mathbf{G}_{\hat{E} \rightarrow E^k}^{-1}$  to compute the triangle  $\hat{T}_i^k$  on the reference element,  $k \in \{m, s\}$ .
    - (D3) Use a two-dimensional quadrature formula to create weights  $\omega_l$  and integration points  $\mathbf{x}_l^m$  and  $\mathbf{x}_l^s$  on the triangles  $\hat{T}_i^m$  and  $\hat{T}_i^s$ , respectively.
    - (D4) Set  $\omega'_l := \omega_l |\det \nabla \mathbf{G}_{\hat{E} \rightarrow E^s}(\mathbf{x}_l^s)| |\hat{T}_i^s|$ .
    - (D5) Add the contribution of triangle  $T_i$ ,

$$b_{pq} \mapsto b_{pq} + \sum_l \omega'_l \hat{\psi}_p(\mathbf{x}_l^s) \hat{\lambda}_q(\mathbf{x}_l^m), \quad p \in \mathcal{N}^s, q \in \mathcal{N}^m,$$

$$d_{pq} \mapsto d_{pq} + \sum_l \omega'_l \hat{\psi}_p(\mathbf{x}_l^s) \hat{\lambda}_q(\mathbf{x}_l^s), \quad p, q \in \mathcal{N}^s.$$

- (C6) End of loop over triangles  $T_i$ .
- (B2) End of loop over master faces  $F^m$ .
- (A3) End of loop over slave faces  $F^s$ .

The one-time creation of the octree in step (A1), which is of complexity  $\mathcal{O}(|\mathcal{N}| \cdot \log(|\mathcal{N}|))$ , guarantees that the remaining steps of the algorithm have optimal complexity  $\mathcal{O}(|\mathcal{N}^s|)$ . For the efficient computation of the intersection  $\tilde{F}^m \cap \tilde{F}^s$  and a Delaunay triangulation in step (C4) we use the quickhull algorithm QHULL [1]. The additionally needed input, a point which is a priori known to lie within the intersection, is computed by a modified simplex algorithm particularly detecting whether an intersection is empty.

We carry out an extensive analysis of our method in context of the numerical simulation of multi-body contact problems in [3]. In particular, we show that our algorithm can be interpreted as an a priori approximation  $\Phi_h$  of the actual (contact) mapping by a composition of local projections and inverse projections. Although, there,  $\Phi_h$  is piecewisely defined and possibly discontinuous at the edges of the slave faces, those considerations close the gap to [8].

Regarding the algorithm as an elaborate construction of an approximate mapping  $\Phi_h$  and subsequent numerical integration in step (D5), we note that the integral is not necessarily evaluated exactly since, in general, the integrand is not a polynomial. An analysis of the additional consistency error due to inexact constraints has

not been achieved yet. But a similar problem arises for the mortar method in case of geometrically matching interfaces if a quadrature rule is used only based on either  $\mathcal{T}^m$  or  $\mathcal{T}^s$ , see [5] and the references therein.

## 4 Numerical Results

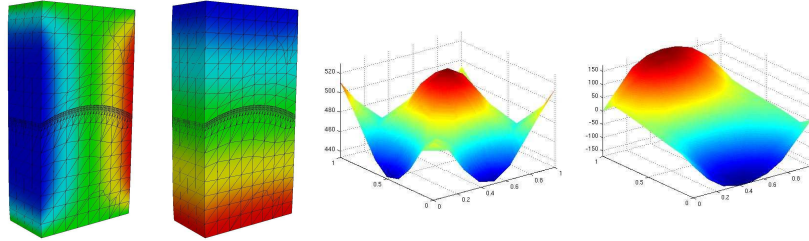


**Fig. 2.** Cut through deformed body with  $u_1$  and  $u_3$ ; normal stresses and one tangential stress component at the non-matching warped interfaces (from left to right).

Our numerical studies, not all presented here, show that the coupling by means of the developed discrete mortar transfer operator results in a discretization with optimal convergence for diverse problem classes and performs very well in various geometrical situations. Here, we consider two vector valued examples from computational mechanics assuming linear elastic material behavior. We are not concerned with complex overall geometries but rather focus on the information transfer across complicated interfaces.

The first example virtually reflects the ideal case where two bodies have to be glued at interfaces coinciding in the continuous setting. In case dual multipliers on warped interior interfaces are used and  $\mathcal{T}^s$  is considerably coarser than  $\mathcal{T}^m$ , the authors in [6] observe artificial oscillations of the deformations as well as the stresses. In contrast, even if  $h_s/h_m \approx 8/1$ , our method yields a smooth solution and does not require any stabilization of the dual multipliers, see Fig. 2. Moreover, one can see that the occurring interface stresses are very well resolved although there are only 81 nodes on the slave side.

As second example we present the numerical solution of a variational inequality arising from a contact problem. Figure 3 shows two separate bodies with bulging interfaces being pressed by non-symmetric Dirichlet boundary conditions at the top and the bottom. Here, for the coupling of the entirely independent hexahedral meshes, which only happens in normal direction, we use standard nodal multipliers and lumping of the matrix  $\mathbf{D}$ . Finally, we note that the computed discrete contact stresses are quite smooth despite the large variations in the local shape of the colliding interfaces.

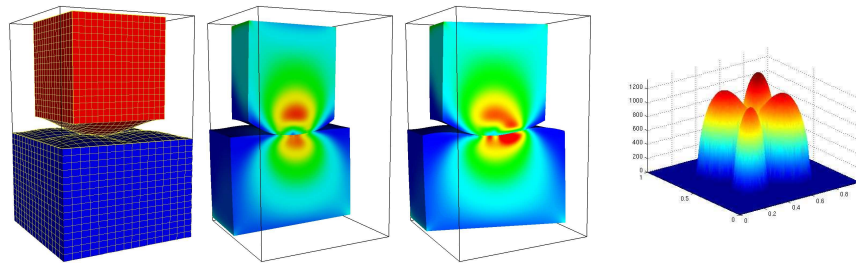


**Fig. 3.** Initial geometry with bulges (left); different cuts through deformed bodies with von Mises stresses (center); normal stresses at contact boundary (right).

## References

- [1] Barber, C.M., Dobkin, D.P., Huhdanpaa, H.: The quickhull algorithm for convex hulls. *ACM Trans. Math. Software*, 22(4):469–483, 1996.
- [2] Bernardi, C., Maday, Y., Patera, A.T.: A new nonconforming approach to domain decomposition: the mortar element method. In H. Brezis and J. L. Lions, eds., *Nonlinear partial differential equations and their applications*, vol. 299 of *Pitman Res. Notes Math.*, pages 13–51. Harlow: Longman Scientific & Technical, New York, 1994.
- [3] Dickopf, T., Krause, R.: Efficient simulation of multi-body contact problems on complex geometries: a flexible decomposition approach using constrained minimization. *Internat. J. Numer. Methods Engrg.*, 2009.
- [4] Eck, C., Wohlmuth, B.: Convergence of a contact-Neumann iteration for the solution of two-body contact problems. *Math. Models Methods Appl. Sci.*, 13(8):1103–1118, 2003.
- [5] Falletta, S.: The approximate integration in the mortar method constraint. In O. Widlund and D. Keyes, editors, *Domain Decomposition Methods in Science and Engineering XVI*, volume 55 of *Lect. Notes Comput. Sci. Eng.*, pages 555–563. Springer, 2007.
- [6] Flemisch, B., Wohlmuth, B.: Stable Lagrange multipliers for quadrilateral meshes of curved interfaces in 3d. *Comput. Methods Appl. Mech. Engrg.*, 196(8):1589–1602, 2007.
- [7] Hüeber, S., Wohlmuth, B.: An optimal a priori error estimate for non-linear multibody contact problems. *SIAM J. Numer. Anal.*, 43(1):157–173, 2005.
- [8] Krause, R., Sander, O.: Fast solving of contact problems on complicated geometries. In R. Kornhuber et al., eds., *Domain Decomposition Methods in Science and Engineering*, vol. 40 of *Lect. Notes Comput. Sci. Eng.*, pages 495–502. Springer, 2005.
- [9] Puso, M.A.: A 3d mortar method for solid mechanics. *Internat. J. Numer. Methods Engrg.*, 59(3):315–336, 2004.